

# Adsorption Kinetics and Thermodynamics of a Malachite Green from Aqueous Solutions by Novel Nanocomposite Hydrogel Ntadbrp-Poly (Aac-Co-Ca)

Marwa R. Nafaa<sup>1</sup> Shaimaa Mohsen Essa<sup>2</sup>

<sup>1,2</sup> Department of Chemistry, College of Education, University of Al-Qadisiyah, Iraq

## Abstract

The adsorption of Malachite green from solution onto the surface of NTADBrP-P(AAC-co-CA) is the subject of this investigation. Although not very effectively, the nanocomposite hydrogels may remove this dye from aqueous solution. At various ionic strength and temperature settings, quantifiable adsorption data have been produced using UV-Visible spectrophotometric method. According to Giles classification, the adsorption isotherms are of the S<sub>4</sub>-curve type, and the experimental data were best suited by the Langmuir and Freundlich isotherm models. The outcomes demonstrate a higher dye adsorption on nanocomposite hydrogels. Temperature effects on the adsorption were studied (15, 20, 25, 30 °C). Malachite green's degree of adsorption on NTADBrP-P(AAC-co-CA) was shown to diminish with rising temperature (exothermic process). The fundamentals of thermodynamics have.

## 1. Introduction

Water pollution is one of the most undesirable environmental problems in the world and it requires solutions. Many different colors, many of which are carcinogenic, mutagenic, and teratogenic as well as hazardous to humans, fish species, and microorganisms, are present in the wastewater produced by the textile industry, which also contains other toxins. Therefore, it is crucial for the ecosystem that they are removed from aquatic wastewater [1,2]. The most frequent pollutants introduced into the aqueous system are dyes. Dyeing is risky, carcinogenic, toxic, and detrimental to the environment, human health, and aquatic ecosystems [3, 4]. 10% to 15% of unneeded dyes are lost to wastewater during the staining or contamination phase, but up to 50% of some reactive dyes are lost during the dyeing process [5]. There are many ways to remove the dye, however using hydrogels to absorb the dye from wastewater is the most practical [6]. When malachite green is released into receiving streams, it affects aquatic life and has a negative impact on the gonads, pituitary gonadotrophic cells, liver, gills, kidney, and intestinal tissues [7]. As a result of the aesthetic effects on receiving waterways, the treatment of wastewater containing such dye is of importance. There have been numerous attempts to remove MG from wastewater. Malachite green can be removed from aqueous solutions using a variety of unconventional sorbents, including de-oiled soya [8], agricultural waste, *Prosopis cineraria* [9], and bagasse. One technology that has attracted a lot of interest is adsorption because of its benefits, including low cost, process flexibility without the formation of sludge, process simplicity, efficiency, and speed [10,11]. Adsorption application ensures

comparatively high efficiency with a straightforward design and straightforward operation. The removal of both organic and inorganic contaminants from aqueous effluents has been widely proposed and accomplished using adsorption techniques utilizing activated carbons. A lot of work has been done recently to propose and use inexpensive adsorbents made from naturally occurring materials and wastes for the removal of dyes from wastewaters because commercially available activated carbons are expensive. The main raw materials being examined for this purpose are agricultural wastes since they are renewable, typically readily available in large quantities, and maybe less expensive [12]. In this study, the crosslinked nanocomposite hydrogel NTADBrP-poly (Acrylic acid -Crotonic acid) was prepared based on the organic reagent prepared in the first using free radical polymerization NTADBrP-P(AAC-co-CA), (MBA) was used as crosslinking agent either as a starter Free radicals (KPS) have been used. The prepared hydrogel and its composites were diagnosed by several techniques including X-ray diffraction (XRD), infrared spectroscopy (FT-IR), emission field scanning electron microscopy (FE-SEM) and TGA techniques, in addition to surface area analysis and the porous nature of the surface (BET, BJH). MG adsorption's response to adsorbent dosage, initial MG concentration, reaction temperature, and pH. Additionally assessed and reported were adsorption kinetics, isotherms, and thermodynamic parameters.

## 2. Materials and Methods

### Instruments

(FTIR)Spectra (4000-400cm<sup>-1</sup>) in KBr disks were recorded on a SHIMADZU FTIR-8400S fourier transform infrared spectrophotometer (Japan),

Visible spectrophotometer, Dunboff metabolic shaking Incubator GCA/ precision Scientific, Centrifuge tubes. pH-Meter.

### Materials

NTADBrP as organic reagent and Crotonic Acid (C.A, 98% ; Reagent World) were use as monomers. N,N-methylene-bis acrylamide ( MPA 99% ; Himedia Laboratories) was used as a crosslinking agent. Potassium persulfate (KPS, 99%; Riedel-dehaenag seclze hannover) was used as an initiator. Acrylic Acid (AAC, 99%; Himedia) was used as accelerator. All these substances were used to the preparation of hydrogel and nanocomposite. Malachite green (MG, 98%; Alpha Chemical) was use a model of dye in adsorption. Hydrochloric acid (HCl, 35%; J.T.Baker) and Sodium hydroxide (NaOH, 98%; Alpha Chemika). Sodium chloride (NaCl 99%; Alpha Chemika) and Deionized water (DI) was use through all the complete experimental in this research.

### 3. Methodology

Preparation of NTADBrP -P(AAC-co-CA) chemically nanocomposite hydrogel

The NTADBrP-Poly (AAC-co-CA) hydrogel complex was prepared from a group of solutions starting by dissolving 0.5 g of CROTONIC ACID in 20 ml of water and stirring continuously for 40 minutes with a HOT PLATE STIRRER magnetic stirrer at laboratory temperature. Then add a solution of the organic reagent with a concentration of (0.01) molar, prepared by dissolving (0.0816) grams of the reagent in 20 ml of absolute ethanol in the form of drops to the CROTONIC ACID solution with constant stirring after that 5 ml of acrylic acid is added, then a solution of potassium persulfate is prepared. KPs by dissolving 0.1 g of it in 2 ml of water, as well as preparing the MPA (N,N - Methylene – Bis acrylamide) binder by dissolving 0.1 g of it in 2 ml of water, The MBA bond (N,N - Methylene – Bis acrylamide) is added with stirring and put N<sub>2</sub> gas for 5 min, then the initiator solution is added initiator potassium persulfate KPS in the form of drops to the solution with stirring, and then we transfer the solution to a water bath at a temperature of 50 °C for 2h to complete the reaction, then take Polymer, washed with distilled water and dried in an electric oven at 60 °C.

### 4. Results and Discussion

#### Fourier Transform Infrared (FT-IR) analysis

The NTADBrP-P(AAC-co-CA) nanocomposite hydrogel before and after the adsorption process. The infrared spectrum shown in the figure below for the superposed showed a wide beam at the range 3379 cm<sup>-1</sup>, which indicates the interference that occurred between the two O-H beams in the carboxyl and hydroxyl group and the N-H group in the MBA crosslinker, and the appearance of a beam at the frequency 2372cm<sup>-1</sup> represents the stretchy

vibrations of the symmetric and asymmetric CH<sub>2</sub>-CH<sub>2</sub> in the aliphatic compounds that exist within the structure, and the 1626cm<sup>-1</sup> band belongs to the carbonyl group C=O found in the carboxylic acid. As for the range (1402-1031 cm<sup>-1</sup>), the absorption bands that appeared are due to the presence of the bonds C-C, C-N, and C-O respectively. The figure below shows the infrared spectrum of the composite before and after the adsorption process of malachite green dye, showed a group of characteristic bands at 1542cm<sup>-1</sup>, 1342cm<sup>-1</sup> and 1164cm<sup>-1</sup> refer to MG dye, where the visible band at 1558cm<sup>-1</sup> refers to group C=C for the benzene ring within the composition of the dye, as well as the infrared spectroscopy of the compound shows the beam shift towards lower wavelengths as the carbonyl group C=O beam shifts from 1626 cm<sup>-1</sup> to 1712 cm<sup>-1</sup>, as a result of the hydrogen bonding that occurs between the adsorbent surface And dye molecules, and this indicates the adsorption of the dye on the surface of the composite[13,14].

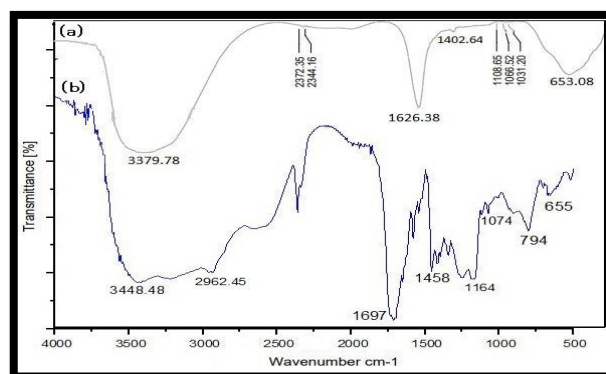


Fig 1: FT-IR for nanocomposite; (a) before adsorption, (b) after adsorption

#### Thermogravimetric analysis (TGA)

Initially dried to a fixed weight in a vacuum oven, NTADBrP-P(AAC-co-CA) nanocomposite hydrogel was then heated at a rate of 10 °C/min from 40 °C to 900 °C to determine thermogravimetric diagrams using TGA (TGA4000, Perkin Elmer, USA).



Fig 2: Thermogram of the NTADBrP-P(AAC-co-CA)

In Fig 2 the results revealed that the compound has a very stable surface at temperatures up to about 220 °C, indicating that it enjoys good temperatures, and that at this range, water molecules or any other

absorbed solvent molecules are lost. This loss was confirmed by the clear decrease in the DTA curve at a temperature of 82 °C and that the percentage of loss is small, about 4.3% , as the dissolution process of the compound occurs in two stages, the first of which is the fission of the compound. The second stage begins with a sharp weight loss at temperatures 340-490 °C, which is attributed to the loss of CO<sub>2</sub> from the structure of the complex. The dissolution rate is significant, at roughly 48.70%, and is caused by the breakdown of crosslinking in the polymeric chains that make up the produced chemical. It was discovered that the reaction is endothermic through the DTA curve [15].

Field Emission scanning electron microscopy (FE-SEM)

Field Emission Scanning Electron Microscopy (FESEM) was used to analyze the nanocomposite hydrogel's surface morphology (Tescan MIRA3, Germany). Analyses of the nanocomposite made of NTADBrP-P (AAC-co-CA). Under low pressure, a small layer of gold was applied to them, and then their FE-SEM pictures were captured.

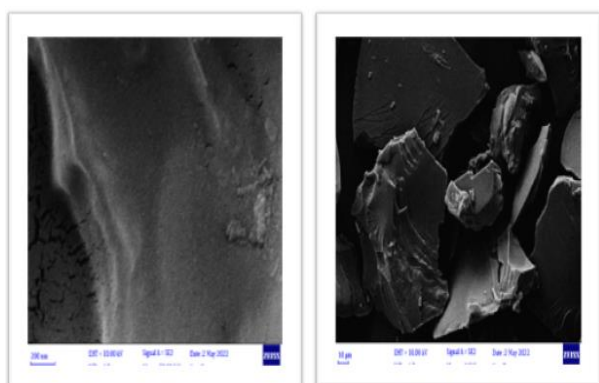


Fig 3: FE-SEM images of NTADBrP-P(AAC-co-CA) nanocomposite hydrogel before adsorption

FE-SEM images in Fig 3 depicting the addition of the NTADBrP reagent to the hydrogel, which produces the composite NTADBrP-P(AAC-co-CA). The external shape of the sample surface displayed an increase in roughness and porosity with an irregular structure, and the reagent particles were distributed uniformly throughout the hydrogel matrix, with no evidence of reagent aggregation. This is caused by the functional aggregates that are present on the surface of both the reagent and the hydrogel, which interact with the hydrogel matrix [16].

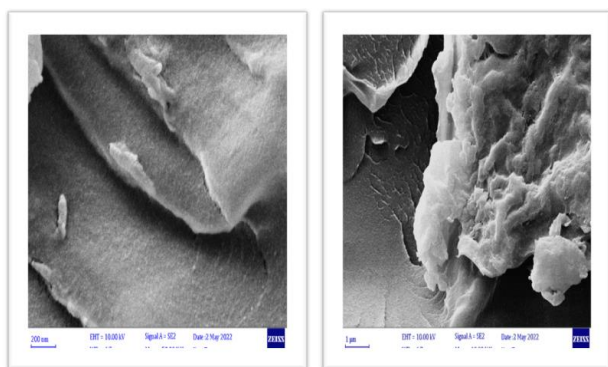


Fig 4: FE-SEM images of adsorption MG dye on NTADBrP-P(AAC-co-CA) nanocomposite hydrogel

The FE-SEM images depicted in the preceding two figures after MG dye adsorption on the surface of the composite demonstrated an improvement in the smoothness of the surface as a result of the dye molecules completely filling the pores on the surface in the form of a layer, and then the surface became completely covered with dye molecules. This confirms the occurrence of adsorption as it is acknowledged in the literature [17].

### Equilibrium time

The impact of equilibrium time was determined by adding 0.05 g of NTADBrP-P(AAC-co-CA) nanocomposite hydrogel to 10 mL of MG dye solution with an initial concentration of 100 mg/L while shaking. The temperature of the solution is maintained at 25°C using thermostatic controls and a shaker. The samples were centrifuged and taken for spectrophotometric analysis to determine the amount of MG dye after varying amounts of time.

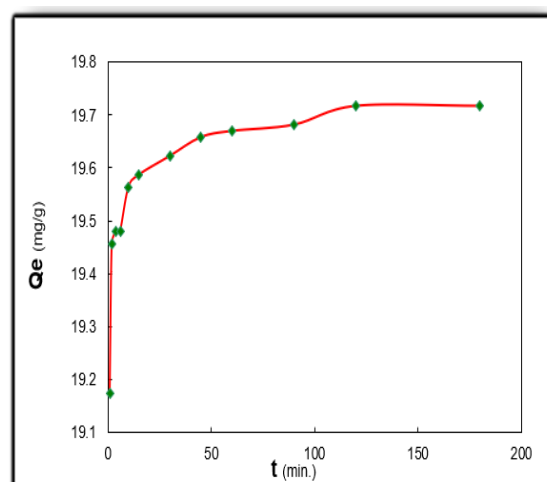


Fig 5: The effect of equilibrium time on adsorption capacity

demonstrates the impact of contact time for initial dye concentration on the elimination of MG by NTADBrP-P(AAC-co-CA). In the first 45 minutes, adsorption happened quickly; after that, it happened more slowly. The adsorption process eventually reached a dynamic equilibrium and the amount of dye adsorbed onto the adsorbent stayed roughly constant. This happened when the amount of dye being adsorbed onto the adsorbent was equal to the amount of dye being desorbed from the adsorbent. Contact time curves showed that the equilibrium took 45 minutes for all dye concentrations. This explains why in the batch equilibrium studies mentioned above, the ideal contact period was 45 minutes. The single, smooth, and continuous curves indicate probable monolayer coverage and eventually to saturation [18].

The maximum wavelength of the MG dye was determined by measuring the ultraviolet-visible absorption spectra of the dye solution (100 mg/L) at wavelengths between 200 and 800 nm. The maximum wavelength of the MG dye solution was

discovered in Fig 6 to be max MG = 622.0 nm.

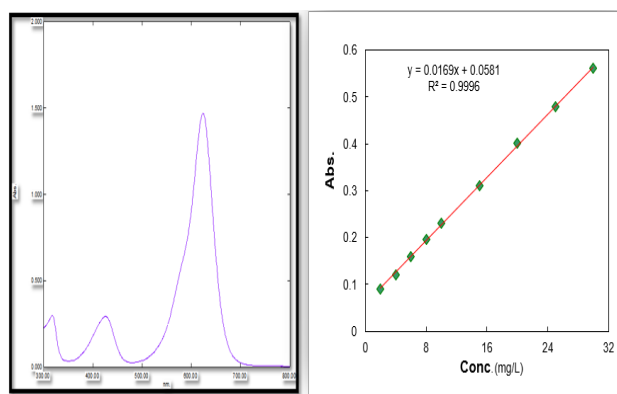


Fig 6. a. UV-Visible absorption spectra and b. Calibration curves of the MG dye

Solutions of different MG dye concentrations created through repeated dilutions. These solutions' absorbance values were measured at the MG dye's chosen max wavelength (622.0 nm), and the results are plotted versus the MG concentration values in Fig 6 b.

### Calculate the Quantity Adsorbed

The following equation [19] can be used to calculate how much MG dye adsorbent is present on the surface of NTADBrP-P (AAC-co-CA) nanocomposite hydrogel.

$$Q_e \text{ or } \frac{x}{m} = \frac{V(C_o - C_e)}{m} \quad (1)$$

Were

x: the quantity adsorbed.

m: weight of adsorbent (g).

Co: initial concentration (mg/L).

Ce: equilibrium concentration (mg/ L).

V: volume of solution (L).

### Effect of Temperature

To estimate the fundamental thermodynamic functions, the adsorption experiment was repeated in the same way at temperatures of 15, 20, 25, and 30 °C. The general shapes of dyes adsorption isotherms at four different temperatures are given in Fig7.

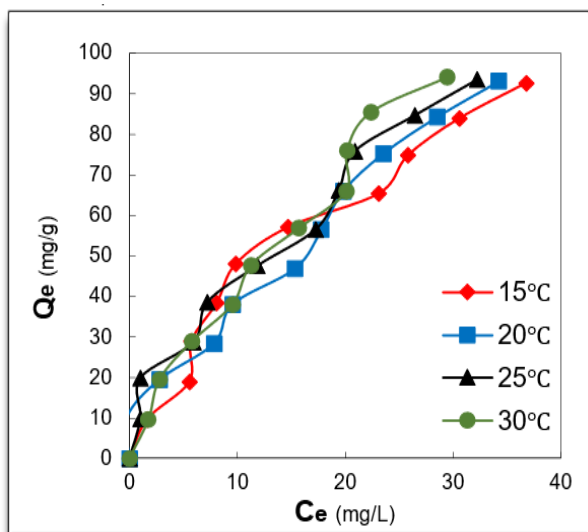


Fig 7: Adsorption isotherms of dyes on composite at

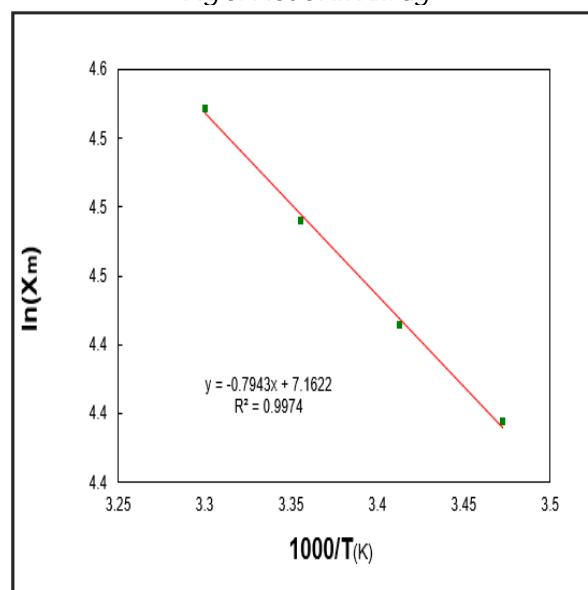
### different temperatures

A number of studies were carried out with various concentrations (50-500 mg/L) and temperatures (30, 25, 20, 15°C). It was evident from the results that the adsorption process intensifies as temperature rises, which suggests that adsorption is exothermic.

The solubility of dye molecules is temperature-dependent, which reinforces the decrease in adsorbate-adsorbent interaction with rising temperatures. The less a molecule's tendency to adsorb onto the surface of the NTADBrP-P(AAC-co-CA) nanocomposite hydrogels, the better it is solvated at higher temperatures. By computing Xm values at various temperatures, the fundamental thermodynamic parameters of dye adsorption on the composite were calculated. The Van't Hoff equation may be used to calculate the heat of adsorption ( $\Delta H$ ):  $\ln X_m = \frac{-\Delta H}{RT} + \text{constant}$ , the change in free energy ( $\Delta G$ ), which can be estimated using the equation ( $\Delta G = -RT \ln K$ ), and the change in entropy ( $\Delta S$ ), which can be calculated using the Gibbs equation. The Gibbs equation ( $\Delta G = \Delta H - T \cdot \Delta S$ ) can be used to calculate the change in entropy ( $\Delta S$ ). Figure (7) and Table (1) provide examples of these calculations.

	Temp.(K)	1000/T(K-1)	Xm	ln(Xm)
Ce 28.6	288	3.472222	82	4.406719
	293	3.412969	85.5	4.448516
	298	3.355705	89.5	4.494239
	303	3.30033	94	4.543295

Fig 8: Plot of ln Xm ag



ainst reciprocal absolute temperature on nanocomposite

The essential thermodynamic values of dye adsorption on NTADBrP-P(AAC-co-CA) are displayed in Table (2). These numbers show that an adsorption of the van der Waals type has occurred.

**Table 2 : Values of thermodynamic functions of adsorption process of dye on the NTADBrP-P(AAC-co-CA) hydrogels at 25 °C**

	$\Delta H(\text{kJ/m ol.})$	$\Delta G(\text{kJ/m ol.})$	$\Delta S(\text{kJ/K.m ol.})$	Equilibrium Constant(K)
M				
G	6.604	-6.700	44.643	15.647

The enthalpy ( $\Delta H$ ) and free energy change ( $\Delta G$ ) values of the dye adsorption on NTADBrP-P(AAC-co-CA) are negative, indicating exothermic and spontaneous adsorption. In addition to a reduction in entropy, the adsorption of dye on nanocomposite is exothermic. This outcome can be explained by the fact that the ordered limited adsorbed layer's entropy change ( $\Delta S$ ) is consistently lower than that of the dissolved solutes. The impact of ionic strength on the dye's adsorption uptake on NTADBrP-P(AAC-co-CA) surface is depicted in Fig 8.

**Effect of Ionic Strength**

Under the same experimental circumstances as previously described, the impact of adding (0.001-0.15g) of sodium chloride, Potassium Chloride and Calcium carbonate to solutions having a fixed concentration of adsorbate and equilibrated with 0.05 g of adsorbent was examined.

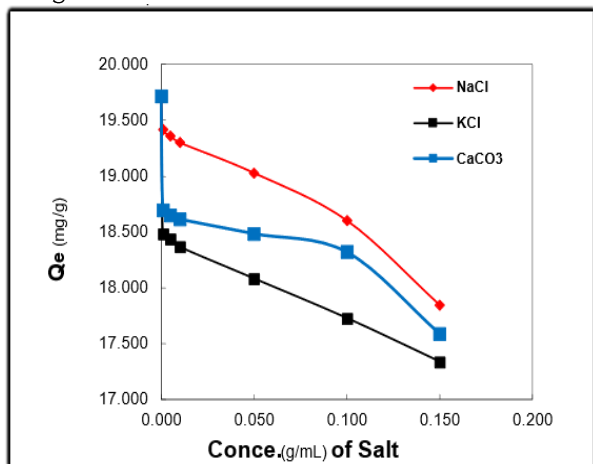


Fig 9: Adsorption isotherms of dye on nanocomposite in the presence of different concentrations of salts at 25 °C

Figures depict a general rise in dye uptake with increasing electrolyte concentration (and hence, ionic strength). This effect might be brought on by a decrease in the solubility of the adsorbate as a result of increased interactions between electrolyte ions and the aqueous solvent. Ionic salts often have a better solubility in aqueous media than do the molecules of organic colors. The attraction between the dye molecules and the nanocomposite surface therefore increases as a result of their competition to interact with the solvent molecules [20].

Researchers have tested the adsorption of dyes from aqueous solutions at 25 °C as well as at 15 °C, 20 °C, and 30 °C on NTADBrP-P(AAC-co-CA). Fig 10 , which plots the quantities adsorbed on composite as a function of equilibrium concentration at the constant temperature, illustrates the general forms of dye adsorption isotherms.

According to the findings, the NTADBrP-P(AAC-co-

CA) adsorptive 's capabilities increased as dye concentration did. The nanocomposite hydrogels' decent surface activity in the adsorption of certain colors from solution was discovered. Malachite green's and NTADBrP-P(AAC-co- CA) adsorption capabilities both rose as the dye concentrations were raised.

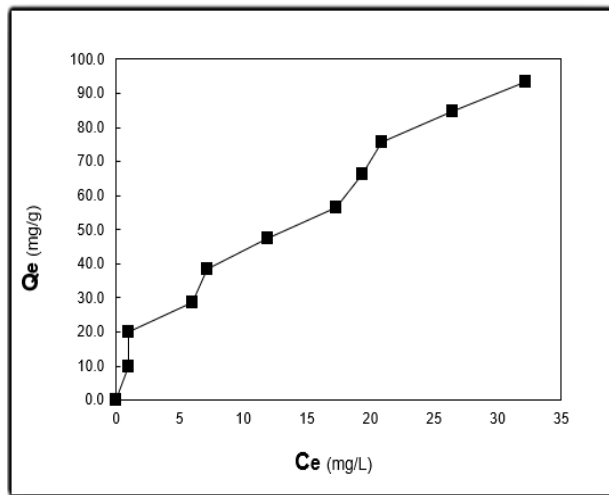


Fig 10: Adsorption isotherms of dyes on the NTADBrP-P(AAC-co-CA) at constant temperature (25 °C)

The Langmuir, Temkin and Freundlich isotherm expressions were used to examine the data from the adsorption equilibrium.

The Freundlich equation provides the most accurate representation of the isotherms that underlie the adsorption of dyes on composite.

$$\frac{x}{m} = K C_e^{1/n} \dots\dots\dots (2)$$

Where  $x/m$  is the quantity adsorbed in mg/g.  $C_e$  is the equilibrium concentration in mg/L,  $n$  and  $k$  are constants for the given adsorbent and solute. The applicability of Freundlich isotherm is indicated by using the linear form of Freundlich equation.

$$\log \frac{x}{m} = \log k + \frac{1}{n} \log C_e \dots\dots\dots (3)$$

Following are several ways to express the Langmuir isotherm.

$$Q_e = \frac{q_m K_L C_e}{1 + K_L C_e} \dots\dots\dots (4)$$

**Where**

- $Q_e$ : amount adsorbed per unit weight of adsorbent at equilibrium (mg/g).
- $C_e$ : equilibrium concentration of adsorbate in solution after adsorption (mg/L).
- $Q_m$  (mg/g) and  $K_L$  (L/mg) are the Langmuir isotherm constants.

The Langmuir isotherm constants are evaluated through linearization of Eq. (4).

$$\frac{C_e}{Q_e} = \frac{1}{q_m K_L} + \left(\frac{1}{q_m}\right) C_e \dots\dots\dots (5)$$

Following are several ways to express the Temkin isotherm.

$$\ln(kT C_e q_e) = \frac{RT}{b} \dots\dots\dots (6)$$

The Temkin isotherm constants are evaluated through linearization of Eq. (5).

$$q_e = B \ln kT + B \ln C_e q_e \dots\dots\dots (7)$$

**where**

$q_e$ : equilibrium adsorption capacity.

T: absolute temperature.  
 B: A constant related to the heat of adsorption (J.mol<sup>-1</sup>).  
 C<sub>e</sub>: equilibrium concentration of adsorbate in solution after adsorption (mg/L).  
 KT: Temkin constant.

Mode I	Equation	Slope	inter.		
Lang.	$y = 0.0078x + 0.1234$	0.0078	0.1234	Q <sub>m</sub>	K <sub>L</sub>
	$R^2 = 0.7966$			128.205	0.063
Frend.	$y = 0.6662x + 0.9695$	0.6662	0.9695	N	K <sub>f</sub>
	$R^2 = 0.974$			1.501	9.322
Temk.	$y = 36.675x - 38.655$	36.675	-38.655	B	K <sub>t</sub>
	$R^2 = 0.9468$			36.675	0.349

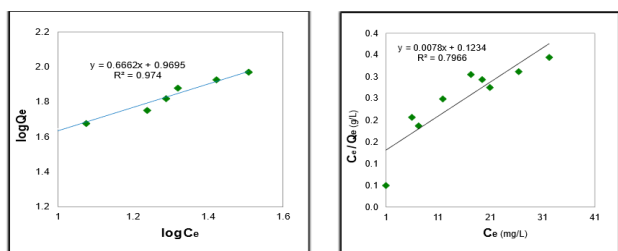


Fig11: Linearized models isotherms of dyes onto polymer at 25°C: a- Freundlich b- Langmuir

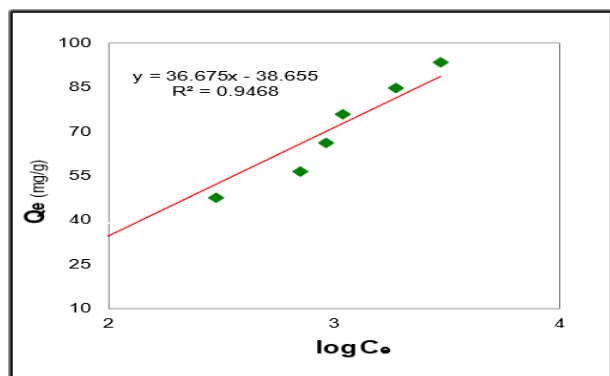


Fig 12: Linearized models isotherms of dyes onto polymer at 25°C: C- Temkin

### Adsorption Kinetic Models

Fig 13 illustrates the results of calculating the time needed to reach the equilibrium state of MG dye adsorption on composite surface as a function of equilibrium time with constant dye concentration at various time intervals (1-180 min) at 25 °C, constant composite weight of 0.05g, and pH 7.0. It takes 45 minutes to reach equilibrium. The rate of adsorption increases over time, beginning with a high rate in the first five minutes and increasing gradually to reach the contact time at 45 minutes. Adsorption is slower and more difficult because all of the active sites on the surface of the adsorbents are filled by dye molecules, which is caused by the high number of accessible adsorption active sites [21]. The adsorption of the dye on the surface made good use of the kinetic models of the adsorption process that adequately reflect the experimental data. The experimental results were analyzed using the kinetic

reaction models. Using fictitious first order and fictitious second order equations, the reaction rate constants of the dye removal from the solution by NTADBrP-P(AAC-co-CA) were computed. The experimental findings were described using the first order rate in the Lagergren equation. The Lagergren equation can be express linearly as [22].

$$\ln(q_e - q_t) = \ln q_e - k_1 t \dots\dots\dots (8)$$

Capacity and q<sub>t</sub> (mg/g) refer to the amount of dye adsorbed at a given time, where q<sub>e</sub> (mg/g) represents the equilibrium adsorption. The slope of the plot of ln(q<sub>e</sub>-q<sub>t</sub>) against t, shown in Fig 8 a, can be used to derive the values of K<sub>1</sub> for the MG-NTADBrP (AAC-co-CA) nanocomposite hydrogel system. Table 4 lists the adsorption kinetic parameters from Fig 8 b. The adsorption data also uses a false second order technique for analysis. The structure of the linear formula is:

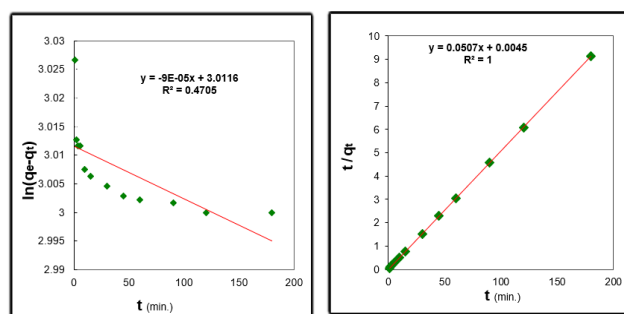


Fig 13: a. Pseudo first order kinetics for adsorption MG b. Pseudo second order kinetics for adsorption of MG

Table 4: Adsorption kinetic parameters of MG on NTADBrP-P (AAC-co-CA) nanocomposite hydrogel for first order and second order

First Order				Second Order			
Slope	intercept	q <sub>e</sub>	R	Slope	intercept	q <sub>e</sub>	R <sup>2</sup>
-9.00E-05	3.0116	0.00009	20.31989	0.4705	0.0507	0.0045	19.72387
						0.51122	222.2222
						0.0507x + 0.0045	
						R <sup>2</sup> = 1	

$$\frac{t}{q_t} = \frac{1}{K_2 q_e^2} + \left(\frac{1}{q_e}\right)t \dots\dots\dots (9)$$

Where K<sub>2</sub> denotes the constant pseudo second order adsorption rate. Equation (10) is as follows when the initial adsorption rate is h = K<sub>2</sub>q<sub>e</sub><sup>2</sup>:

$$\frac{t}{q_e} = \frac{1}{h} + \left(\frac{1}{q_e}\right)t \dots\dots\dots (10)$$

Fig 8 shows how to draw t/q<sub>t</sub> against t to obtain a straight line and calculate q<sub>e</sub>, k<sub>2</sub>, and h [23].

Table 4 contains the adsorption kinetic parameters from Fig 8 as well as the computed kinetic coefficients and correlation coefficients (R<sup>2</sup>) for the two models. According to the findings, the false pseudo-second order equation model had a higher correlation coefficient (R<sup>2</sup>) value than the false pseudo-first order equation. When compared to the amount of the absorbed substance computed in the pseudo first order equation model, the dye absorption calculated in this model is extremely close to the value calculated in the experiments [24].

### 5. Conclusions

The NTADBrP-P(AAC-co-CA) could be employed as

adsorbent in wastewater treatment for the removal of Malachite green from aqueous solution.

The experimental results show that the adsorption equilibrium time was attained in less than 45 minutes.

The kinetic of MG adsorption followed pseudo – first and second - order rate expressions and demonstrated that intraparticle diffusion plays a significant role in the adsorption mechanism.

The hydrogel NTADBrP-P(AAC-co-CA) nanocomposite might be employed as adsorbents to remove MG dye from wastewater. Up to 220 °C, the nanocomposite hydrogel is remarkably stable

#### References

- Ismail, Muhammad, et al. Pollution, toxicity and carcinogenicity of organic dyes and their catalytic bioremediation. *Current pharmaceutical design*, 2019, 25.34: 3645-3663.
- Tang, Hu; Zhou, Weijie; Zhang, Lina. Adsorption isotherms and kinetics studies of malachite green on chitin hydrogels. *Journal of hazardous materials*, 2012, 209: 218-225.
- Subhan, Hanif, et al. Sodium alginate grafted hydrogel for adsorption of methylene green and use of the waste as an adsorbent for the separation of emulsified oil. *Journal of Water Process Engineering*, 2022, 46: 102546.
- Xi, Huan, et al. Highly effective removal of phosphate from complex water environment with porous Zr-bentonite alginate hydrogel beads: Facile synthesis and adsorption behavior study. *Applied Clay Science*, 2021, 201: 105919.
- Perez-Calderon, John; Santos, M. Victoria; Zaritzky, Noemí. Synthesis, characterization and application of cross-linked chitosan/oxalic acid hydrogels to improve azo dye (Reactive Red 195) adsorption. *Reactive and Functional Polymers*, 2020, 155: 104699.
- Velazco-Medel, Marlene A., et al. Cross-Linked Polymer-Based Adsorbents and Membranes for Dye Removal. In: *Membrane Based Methods for Dye Containing Wastewater*. Springer, Singapore, 2022. p. 263-289.
- Sharma, Gaurav, et al. Applications of nanocomposite hydrogels for biomedical engineering and environmental protection. *Environmental chemistry letters*, 2018, 16.1: 113-146.
- Sundararaman, T. R., et al. Adsorptive removal of malachite green dye onto coal-associated soil and conditions optimization. *Adsorption Science & Technology*, 2021, 2021.
- Bharathi, K. S.; Rahesh, S. T. Removal of dyes using agricultural waste as low-cost adsorbents: a review. *Applied Water Science*, 2013, 3.4: 773-790.
- Joshi, Pratiksha, et al. Adsorptive removal of multiple organic dyes from wastewater using regenerative microporous carbon: Decisive role of surface-active sites, charge and size of dye molecules. *Chemosphere*, 2022, 136433.
- Jv, Xiaojun, et al. Fabrication of a magnetic poly (aspartic acid)-Poly (acrylic acid) hydrogel: Application for the adsorptive removal of organic dyes from aqueous solution. *Journal of Chemical & Engineering Data*, 2019, 64.3: 1228-1236.
- Yu, Shujun, et al. Mxenes as emerging nanomaterials in water purification and environmental remediation. *Science of The Total Environment*, 2021, 152280.
- AL-hossainy, Ahmed F.; Abdelaal, Reda M.; El sayed, Wesam N. Novel synthesis, structure characterization, DFT and investigation of the optical properties of cyanine dye/zinc oxide [4-CHMQI/ZnO] C nanocomposite thin film. *Journal of Molecular Structure*, 2021, 1224: 128989.
- Mohsen, Shaimaa, Essa; Hindawi, Wisam ,Hoidy. Spectrophotometric Determination of Cobalt (II) and Lead (II) Using (1,5-Dimethyl-2-Phenyl-4-((2,3,4-Trihydroxy Phenyl) Diazenyl)-1H-Pyrazol-3(2H)-One) as Organic Reagent: Using It as Antimicrobial and Antioxidants, *Nano Biomed Eng*, 2020, 12(2): 160-166.
- Kappe, C. Oliver. Controlled microwave heating in modern organic synthesis. *Angewandte Chemie International Edition*, 2004, 43.46: 6250-6284.
- Nandiyanto, Asep Bayu Dani, et al. Mesopore-free hollow silica particles with controllable diameter and shell thickness via additive-free synthesis. *Langmuir*, 2012, 28.23: 8616-8624.
- Loo, Wei Wen, et al. Enhancement of photocatalytic degradation of Malachite Green using iron doped titanium dioxide loaded on oil palm empty fruit bunch-derived activated carbon. *Chemosphere*, 2021, 272: 129588.
- Gupta, V. K., et al. A comparative investigation on adsorption performances of mesoporous activated carbon prepared from waste rubber tire and activated carbon for a hazardous azo dye—Acid Blue 113. *Journal of hazardous materials*, 2011, 186.1: 891-901.
- Atkins, P.; de paula, J.; Keeler, J. *Molecular Spectroscopy*. Atkins' Physical Chemistry. 2018.
- Ngulube, Tholiso, et al. An update on synthetic dyes adsorption onto clay-based minerals: A state-of-art review. *Journal of environmental management*, 2017, 191: 35-57.
- Wang, Jingyi, et al. red mud derived facile hydrothermal synthesis of hierarchical porous  $\alpha$ -Fe<sub>2</sub>O<sub>3</sub> microspheres as efficient adsorbents for removal of Congo red. *Journal of Physics and Chemistry of Solids*, 2020, 140: 109379.
- Zhao, Guixia, et al. Sorption of heavy metal ions from aqueous solutions: a review. *The open colloid science journal*, 2010, 4.1.
- Warzkiewicz, Monika; Hubicki, Zbigniew. Removal of tartrazine from aqueous solutions by strongly basic polystyrene anion exchange resins. *Journal of Hazardous Materials*, 2009, 164.2-3: 502-509.
- Onuegbuzie, Anthony J.; daniel, Larry G. *Uses and misuses of the correlation coefficient*. 1999.